

0173

Public reporting burden for this collection of information is estimated to average 1 hour per response, including the time for reviewing the data needed, and completing and reviewing this collection of information. Send comments regarding this burden estimate or any other aspect of this collection of information, including suggestions for reducing this burden to Department of Defense, Washington Headquarters Services, Directorate for Information Operations and Reports, 1215 Jefferson Davis Highway, Suite 1204, Arlington, VA 22202-4302. Respondents should be aware that notwithstanding any other provision that may appear in this notice, it does not display a currently valid OMB control number. PLEASE DO NOT RETURN THIS FORM TO THE ABOVE ADDRESS.

1. REPORT DATE (DD-MM-YYYY) 05-04-2005		2. REPORT TYPE Final Report		3. DATES COVERED (From - To) 01-06-2003 - 31-11-2004	
4. TITLE AND SUBTITLE (HBCU/MI) Development of Cumulant-Based Analysis for the Transient Analysis of Stochastic Systems				5a. CONTRACT NUMBER	
				5b. GRANT NUMBER F49620-03-1-0310	
				5c. PROGRAM ELEMENT NUMBER	
6. AUTHOR(S) Timothy I. Matis, Ph.D.				5d. PROJECT NUMBER	
				5e. TASK NUMBER	
				5f. WORK UNIT NUMBER	
7. PERFORMING ORGANIZATION NAME(S) AND ADDRESS(ES) New Mexico State University Office of Grants and Contracts P.O. Box 30001, MSC 3699 Las Cruces, NM 88003-8001				8. PERFORMING ORGANIZATION REPORT NUMBER	
9. SPONSORING / MONITORING AGENCY NAME(S) AND ADDRESS(ES) Neal Glassman Koto White AFOSR/NM AFOSR/PIE 4015 Wilson Blvd. 4015 Wilson Blvd. Mail Room 713 Mail Room 713 Arlington, Va 22203-1954 Arlington, Va 22203-1954				10. SPONSOR/MONITOR'S ACRONYM(S) NM/PIE	
				11. SPONSOR/MONITOR'S REPORT NUMBER(S)	
12. DISTRIBUTION / AVAILABILITY STATEMENT Approved for public release, distribution unlimited					
13. SUPPLEMENTARY NOTES					
14. ABSTRACT This final performance report describes key developments made in the theoretical and applied aspects of using moment closure methods in the analysis of large scale stochastic networks. Areas of primary development include 1) the creation of a self-contained Mathematica [®] package with a users manual that provides moment closure approximations for large stochastic networks, 2) the development of analytical procedures to check for network stability, 3) the development of an optimal truncation policy based on the maximal order of polynomial intensity (rate) functions for the network, 4) a conceptual correlation measure of the error between the accuracy of moment closure approximations and the traffic intensity of the network, and 5) the application of moment closure methods to the sortie generation process.					
15. SUBJECT TERMS					
16. SECURITY CLASSIFICATION OF:			17. LIMITATION OF ABSTRACT	18. NUMBER OF PAGES 51	19a. NAME OF RESPONSIBLE PERSON Timothy I. Matis
a. REPORT	b. ABSTRACT	c. THIS PAGE			19b. TELEPHONE NUMBER (include area code) 505-646-2957

20050519 110

INTRODUCTION

This final progress report details key theoretical and applied advancements in the field of Moment Closure discovered through the course of this project. Specifically, the objective of this work was to study the application of moment closure methods under cumulant truncation to the transient analysis of the sortie generation process. The work that was originally proposed included 1) investigating the accuracy of moment closure procedures, 2) developing procedural improvements to increase accuracy, and 3) applying these to the sortie generation process. As the work progressed, it became apparent that these original objectives needed to be augmented to accomplish the proposed work. As such, additional research objectives of this project include 4) creating a computationally efficient moment closure program and 5) investigating the stability of moment closure methods.

As a result of this work, the following main accomplishments have been achieved 1) the creation of a self-contained Mathematica package with users manual that provides moment closure approximations for large stochastic networks, 2) the development of analytical procedures to check for network stability, 3) the development of an optimal truncation policy based on the maximal order of polynomial intensity (rate) functions for the network, 4) a loose correlation measure of the error between the accuracy of moment closure approximations and the traffic intensity of the network, and 5) the application of moment closure methods to the large-scale sortie generation process. Each of these accomplishments will be discussed individually in the body of the report. There have been three research publications developed as part of this work, two invited presentation, and two contributed presentations. At the present time, a paper titled "" is in the process of being re-submitted to Naval Research Logistics.

RESEARCH FINDINGS

Creation of Moment Closure Program

At the beginning of this project, the Mathematica® program initially authored by the PI for the analysis of stochastic systems was deemed to be inefficient for analyzing large stochastic systems, such as the sortie generation process.

As an example, a 10-node version of the sortie generation model described in Dietz[1] would take several hours to enter and would not fully evaluate due to memory constraints. This same model, however, can be entered and evaluated in a matter of minutes using the streamlined code that was developed through this project.

The process of streamlining the moment closure code was ongoing throughout this project. Significant milestones include the completion of a preliminary streamlined version in April 2004, the completion of a user-friendly version of this code in August 2004, and the ultimate packaging of this code in March 2005. This program provides for the efficient analysis of arbitrarily large networks and only requires user to input the intensity functions of the network, the desired truncation level, and the time horizon over which the model is to be evaluated. The contents of the Mathematica package may be found in Appendix A of this report, a users manual in Appendix B, and a sample implementation in Appendix C. This Mathematica code may be retyped and saved as a .m package file, or an electronic version may be obtained from <http://web.nmsu.edu/~tmatis>. The majority of the coding work was performed by Karl Adams and Ivan Guardiola under the direction of the PI, and the users manual was co-authored by Amara Nance and the PI.

Stability of Moment Closure Methods

"Moment Closure" is a method used in order to close the open set of Differential Equations obtained from the transition intensities using the Random Variable technique that define the moments of the system. Currently two forms of closure are being implemented throughout the scientific community. These two forms of closure are neglect and parametric. Under the closure method of "neglect" we draw to the assumption that all moments and cumulants above a certain "closure level" are insignificant in the sense that they are not vital in order to approximate the low order cumulants of interest. The closure method of "parametric" is done by making an assumption of the underlying statistical distribution and formulating the high order moments and cumulants in terms of the lower ones. The underlying statistical distribution gives us an insight into how the high order moments should be approximated. For example, by making the assumption that the underlying distribution is "Poisson" we would set the high order moments and cumulants above $n > 2$ to be equal to the first

cumulant, this is due to the characteristics of the Poisson distribution. These parametric assumptions allow us to use stability analysis to fully interpret the system's solutions both in transient as well as in steady state.

Stability analysis consists of the deriving the system's stationary points otherwise known as the critical points or equilibrium points of the system. This is done by solving the system of differential equations after the parametric assumption is made in the same manner as solving a linear system of equations. A brief mathematical procedure summary consists of finding the critical points of the system of equations, deriving the Jacobian Matrix at each of the stationary points, deriving the Eigensystem, which contains both the Eigenvalues and Eigenvectors of the system at each point, and deriving a starting point for manifolds that will divide the phase portrait into feasible and unfeasible regions. The procedure above can be done by choosing the appropriate closure of the high order moments and cumulants based on an underlying statistical distribution assumption and setting the differentials to zero. This will yield the corresponding critical points of the system. Stability analysis continues by then giving a description and classification of the system's critical points. The Jacobian of the system will then give us a means of obtaining such classification of the critical points as "source," "sink," or "saddle". Consider the following system

$$\frac{dx}{dt} = f(x, y)$$

$$\frac{dy}{dt} = g(x, y)$$

Looking at this system asymptotically we set the differentials to 0. Thus,

$$0 = f(x, y), 0 = g(x, y)$$

We then find the equilibrium or critical points of the system. Suppose that (x_o, y_o) is an equilibrium point. Then let,

$$J = \begin{bmatrix} \frac{df}{dx}(x_o, y_o) & \frac{df}{dy}(x_o, y_o) \\ \frac{dg}{dx}(x_o, y_o) & \frac{dg}{dy}(x_o, y_o) \end{bmatrix}$$

be the Jacobian Matrix evaluated at the equilibrium point (x_o, y_o) . The Eigenvalues are obtained by solving $\text{Det}(J - \lambda I) = 0$ in terms of λ . The Eigenvalues allow us to fully explore and classify the equilibrium points. These classifications can be determined if the Eigenvalues follow

the following criterion. If the Eigenvalues of the Jacobian matrix are negative real numbers or complex numbers with negative real parts, then the equilibrium point of the system is classified as a stable "sink" or "spiral sink." This solution will approach this point as $t \rightarrow \infty$. If the Eigenvalues are positive or complex with positive real parts then this solution will move away from this point as $t \rightarrow \infty$. Thus, such a point is an unstable point. The point can then be classified as a "source" or "spiral source." If the Eigenvalues are positive and negative parts then this point is classified as a "saddle."

Manifolds are solutions of the system of differential equations which determine the behavior of solutions, within all feasible space. These manifolds are of importance do to the fact that the behavior of solution on either side differ. For example, on one side of the manifold solutions will tend to a stable equilibrium point, where as, on the other side solutions might tend to some infinite value. Therefore, manifolds will be employed in order to separate the phase portrait into feasible and unfeasible regions. The following example considers a single node (compartment) Markov system. Let the immigration/birth rate function be given by $f_1(X) = \lambda = 4$, and let the death rate function be given by $f_{-1}(X) = \mu x^2 = 2x^2$. The system is graphically depicted as



We find the following results for the stability of the above system under a normal and Poisson parametric assumption, yielding the following closure procedures.

Normal Distribution: $k_i(t) = 0 \quad \forall i \geq 3$

Poisson Distribution: $k_i(t) = k_j(t) \quad \forall i, j \geq 1$

Phase plots for these systems are given in Figures 1 and 2.

The results of stability analysis in moment closure approximations are important for various reasons. First, through this analysis we are able to determine a domain for initial conditions in which solutions will behave in accordance to the birth death model characteristics and expectations. This domain determines which initial conditions will yield relevant results and even determine whether solutions can be attained or not. Through a study

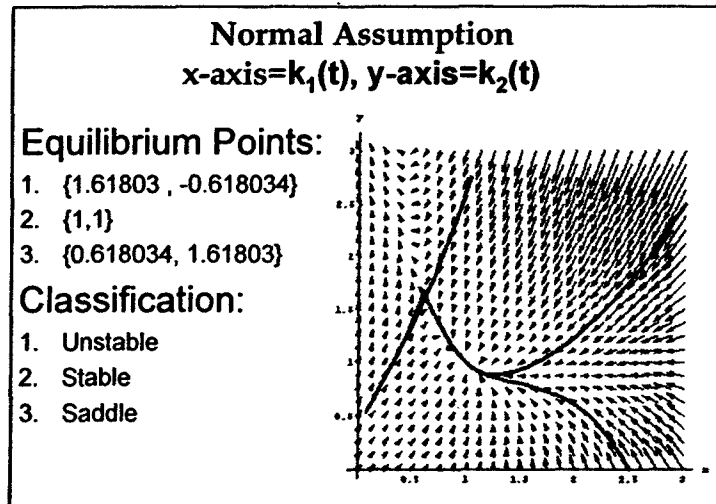


Figure 1: Stability Analysis under a Normal Assumption

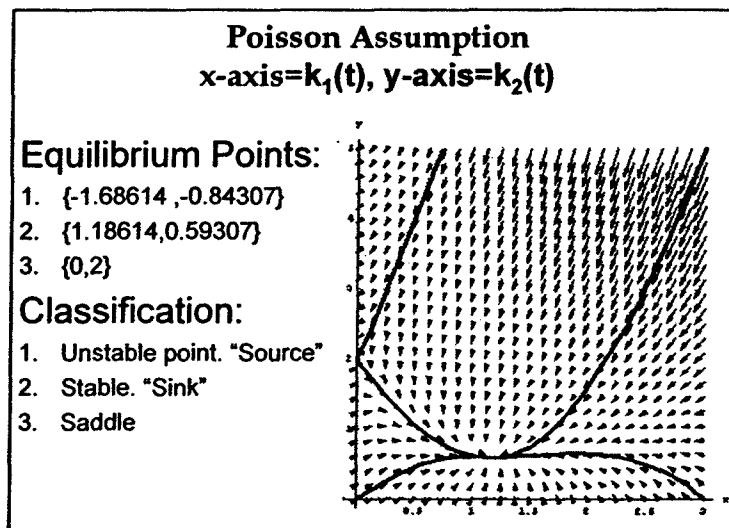


Figure 2: Stability Analysis under a Poisson Assumption

of manifolds we are able to graphically interpret such a domain as shown in the previous figures. The manifolds act as separators of solutions behavior from one side to another we can clearly see that the solution tend toward very different values. This analysis shows us another mode of establishing error involved with the approximation method based on making certain parametric assumptions. This is an important aspect that has not been fully explored by any others in the scientific community. Moment Closure methods are currently being employed in turbulence air flow models, signal processing and many other in which people are employing the moment closure method specific to

parametric assumptions. These parametric assumptions should be under full exploration and determination of system behavior prior to implementation of closure under such assumptions. We explore this issue in order to assure that certain assumption carry certain error, stability and solution behavior.

Optimal Truncation Policies

The accuracy of low-order cumulant approximations, namely mean and variance, under cumulant-neglect moment closure methods will approach the exact values as the level of truncation goes to infinity. Since the computational effort is positively related to the level of truncation, however, our objective was to find a policy that minimizes the level of truncation while maintaining reasonable approximation accuracy. Our mathematical and empirical findings suggest that there are two such 'logical' truncation levels.

In particular, let "s" be the highest order of the intensity function, and "i" be the number of cumulants which we wish to estimate. It follows that "s+i-1" would be the smaller of the two truncation levels and "2s" would be the larger of these. The lower truncation level accounts for all cumulants that are in the associated differential equations generated by the system, and the higher level includes those cumulants that are one order removed. Truncating below the lower level leads to significant approximation error, while above the upper leads to unnecessary computational effort.

We present numerical results to summarize the above truncation scheme for High, Medium and Low traffic situations in Figures 3-8. In all in each case, the maximum order of the arrival and service intensities were quadratic and our objective is to estimate the Mean and Variance of the system. Hence, it follows that the minimum truncation level is $(2+2-1)=3$, and the Maximum Truncation level is $(2*2)=4$. We observe that mean is quite well approximated under the Low, Medium and High traffic intensities. The approximation accuracy of the variance, however varies. In particular, the variance is under-approximated under the lower truncation limit and over-approximated under higher truncation limit under the varying traffic intensities.

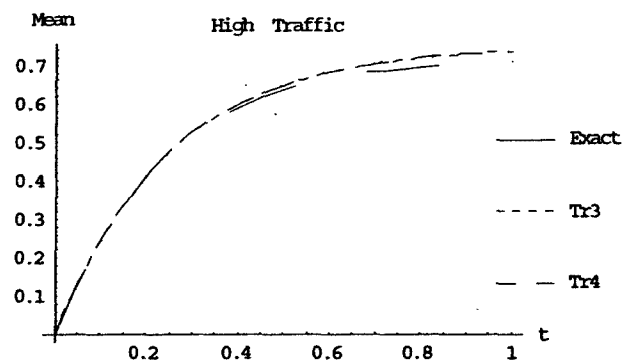


Figure 3: Mean Approximations under High Traffic

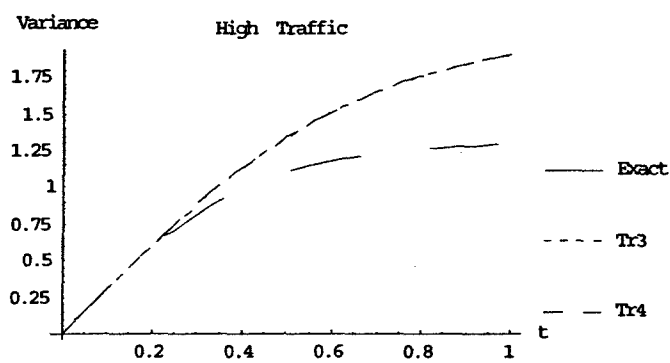


Figure 4: Variance Approximations under High Traffic

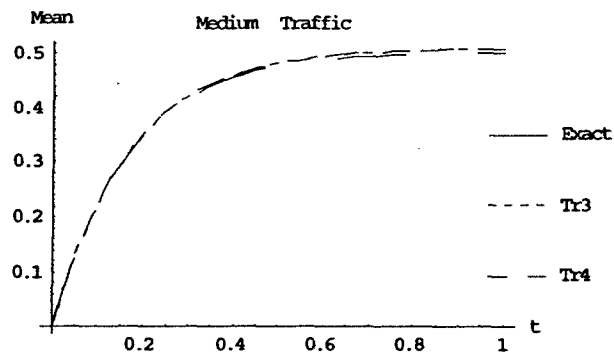


Figure 5: Mean Approximations under Medium Traffic

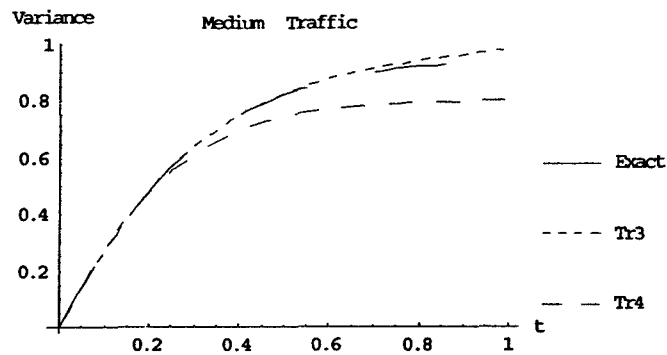


Figure 6: Variance Approximations under Medium Traffic

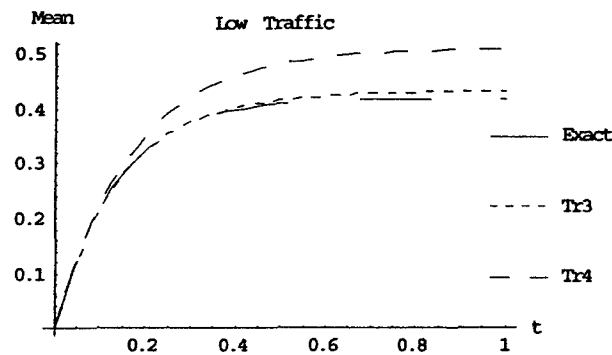


Figure 7: Mean Approximations under Low Traffic

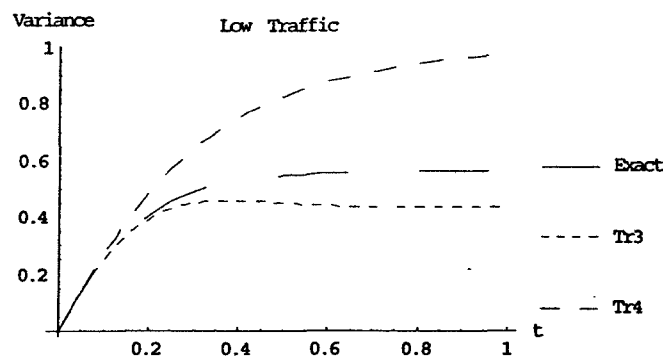


Figure 8: Variance Approximations under Low Traffic

Effect of Traffic Intensities on Approximation Accuracy

Investigations into optimal truncation policies lead to the observation that the traffic intensity greatly affects that accuracy of the moment closure approximations. In particular, empirical evidence indicates that the accuracy of the approximations is best for medium traffic systems and deteriorates as we move to low and high traffic systems. This finding is dependent on the systems under

study, yet holds for a large body of models. A graphically illustration of this is given in Figure 9. To study the effect of traffic intensity, we consider a single node system with 2nd order polynomial intensities. Generating exact solutions for the low-order order cumulants of the system via Kolmogorov equations, we noticed that in general the 4th order cumulant was large under low traffic, small under medium traffic, and very large under high traffic. It follows that under 3rd order truncation, this potentially large term may be missing from the equation. The effect of this and other large higher-order cumulants may propagate through as the truncation level is increased. This aspect of the project remains in the exploratory stages, yet is an area that warrants future research attention.

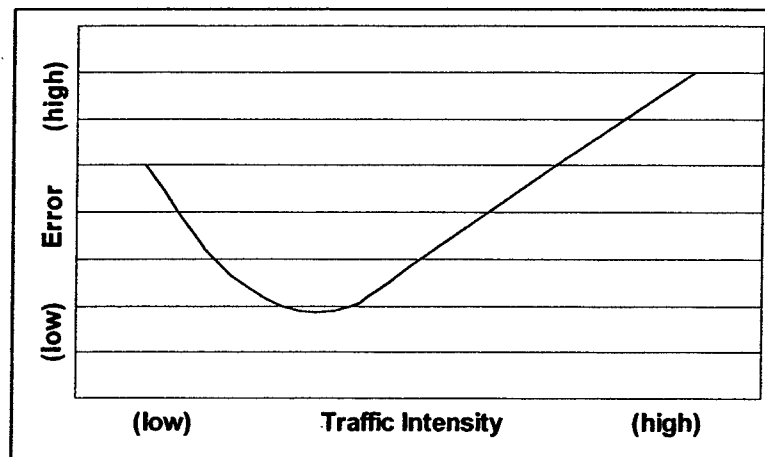


Figure 9: Traffic Intensity and Approximation Error

Analysis of the Sortie Generation Process

Moment Closure methods, under a cumulant-neglect policy, were applied to the sortie generation model. The model considered mimicked that of Dietz[1]. A paper on this subject was written and submitted to Naval Research Logistics, yet is presently under revision for a resubmission. The original draft of this paper is included in Appendix D, in which a Phase-type distribution is used to model the fork-join nodes.

RESEARCH MATERIALS

The following research publications were developed under this grant.

- Jayaraman, R., Matis, T. and Guardiola, I. (2004) "Effect of Polynomial Intensity Functions on Cumulant Derivation Procedures", Proceeding of the 2004 Industrial Engineering Research Conference.
- Matis, T. I. and Kharoufeh J. P., (2005) "Transient Queueing Network Analysis of Sortie Generation" Naval Research Logistics (under revision).
- Matis, T. and Guardiola I. (2005) "On the Stability of Moment Closure Methods" Operations Research Letters (in preparation).

This work was presented at several research conferences, including

- Stability Region Identification for Non-Linear Stochastic Systems Using Moment Closure Methods, Institute for Operations Research and the Management Sciences 2004 Annual Conference, Denver, Colorado, October 2004
- Jayaraman R., Matis T. I., and Guardiola I. (2004) "Effect of Polynomial Intensity Functions on Cumulant Derivation Procedures", Proceedings of the Institute of Industrial Engineering 2004 Annual Conference.

CONCLUSION

The research performed under this grant has lead to significant advancements in the theoretical and applied aspects of Moment Closure methods. Notable theoretical advancements include documented studies on the stability, accuracy, and optimality of moment closure methods, and applied advancements include efficient computational routines for analyzing large systems and demonstration of applicability to the sortie generation process. A website at <http://enr.nmsu.edu/~tmatis> contains copies of computational codes, papers, and presentation produced under this grant.

REFERENCES

- [1] Dietz, D. and Jenkins R. (1997) "Analysis of Sortie Generation with the Use of a Fork-Join Model", *Naval Research Logistics*, Vol. 44, pp. 153-164

APPENDIX A
MOMENT CLOSURE MATHEMATICA® PACKAGE
(MCP.m)

```
(*****
*****
```

This file is intended to be loaded into the Mathematica kernel using the package loading commands Get or Needs.

```
*****
*****)
```

```
(*This Notebook is the keeper of all function which are
necessary in order to \
evaluate a give node system using transient analysis
corresponding to moment \
neglect*)
```

```
(*Packages needed in order to use this program*)
(*Wirtten by Ivan Guardiola &Tim Matis*)
<<DiscreteMath`Combinatorica`
<<momcum.m
```

```
(*This function build the left hand side of the of the
partial differential \
equations.*)
LHSPDE[Nodes_,TRUNC_]:=
```

```
Module[{AA,AB,AC,AD,AE,AF,AG,AH,AI,AJ,AK,AL,AM,AN,AO,AP,AQ,
AR,AS,AT,AU,AV,
ORLI,MGFList,CGFlist,IVV,mgfl,Cgf, MGF,LHSpde},
```

```
AA=Table[Table[0,{Nodes}],{Nodes}];AB=MapThread[K,Transpose
[AA]];
AC=MapThread[m,Transpose[AA]];Clear[AA];
```

```
AD=AB/.{K[b__]\[Rule]K[b][t]};AE=Take[First[AD]];AF=Take[Fi
rst[AC]];
```

```
Evaluate[AE]==0;Evaluate[AF]==1;AG={a,b,c,d,e,f,g,h,r,s,t,u
,v,w,x,y,z};
```

```
AH=Take[AG,Nodes];AI=Table[0,{Nodes}];AJ=Table[TRUNC,{Nodes
}];
```

```
AK=Transpose[{AH,AI,AJ}];AL=MapThread[m,AH,0];AM=MapThread[
K,AH,0];
```

```
AN=Table[Subscript[\[Theta],i],{i,Nodes}];AO=AN^AH;AP=Times
@@AO;
```

```

AQ=Factorial[AH];AR=Times@@AQ;

AS=AP/AR;AT=AM/.{K[z__]\[Rule]K[z][t]};AU=AL*AS;AV=AT*AS;
(m[i__]/;Plus@@{i}\[GreaterEqual]TRUNC+1)=

0;(K[i__][t]/;Plus@@{i}\[GreaterEqual]TRUNC+1)=0;ORLI={};
For[i=1,i<TRUNC+1,
  If[i\[Equal]1,AppendTo[ORLI,Compositions[i,Nodes]],
    AppendTo[ORLI,Join[ORLI[[i-
1]],Compositions[i,Nodes]]];i++];
orderList1=Last[ORLI];ORLI={};MGFList={};CGFList={};
For[i=1,i<Length[orderList1]+1,
  IVV=Thread[AH\[Rule]orderList1[[i]]];
  AppendTo[MGFList,AU/.IVV];

AppendTo[CGFList,AV/.IVV];i++];mgf1=1+Plus@@MGFList;Cgf=Plu
s@@CGFList;
MGF=Exp[Cgf];
LHSpde=D[MGF,{t,1}]/.{\[ExponentialE]^Cgf
\[Rule]mgf1};{LHSpde, MGF,Cgf,
  mgf1}
]

(*This function builds and evaluates all necessary
symbolics in order to \
create the right hand side of the partial differential
equations*)
EQUATE[F_,B_,TRUNC_]:=

Module[{F2,Y,Y2,Y5,Y7,Nodes,AN,AG,AH,ord,Y8,Y11,ORLI,orderL
ist1,

relationsmod,relations,momcumrule,AO,T1,Y12,LHL,LHSpde,MGF,
Cgf,mgf1,stu,
  butt,butt2},F2=Partition[F,1];
Nodes=Length[B[[1]]];
Y=Table[Join[Take[F2[[i]]],Take[B[[i]]]],{i,1,
  Length[F]}/.{Plus\[Rule]List};
Y2=Partition[
  Flatten[Table[
    If[ListQ[Y[[i,1]]]\[Equal]False,Y[[i]],
Table[{Flatten[Y[[i,1]]][[j]],Drop[Y[[i]],1]},{j,1,
Length[Y[[i,1]]]}]],{i,1,Length[Y]}],1+Length[B[[1]]];

```

```

Y5=Y2/.Thread[Variables[F]\[Rule]Table[1,{Length[Variables[F]]}]]];
  AN=Table[Subscript[\[Theta],i],{i,Nodes}];

AG={a,b,c,d,e,f,g,h,r,s,t,u,v,w,x,y,z};LHL=LHSPDE[Nodes,TRUNC];

LHSpde=LHL[[1]];MGF=LHL[[2]];Cgf=LHL[[3]];mgf1=LHL[[4]];AH=Take[AG,Nodes];

Y7=Table[Y5[[i,1]]*Sum[(Plus@@(AH*AN))^j/j!,{j,1,TRUNC}]/.Thread[
  AH\[Rule]Take[Y2[[i]],{2,2+Length[B[[1]]]-1}]],{i,1,Length[Y5]}];

ord=Table[Exponent[Y2[[i,1]],Variables[F]],{i,1,Length[Y2]}];

Y8=Table[Prepend[Table[{AN[[j]],ord[[i,j]]},{j,1,Length[ord[[i]]]}],
  MGF],{i,1,Length[Y5]}];

Y11=Plus@@(Y7*(Table[D@@Y8[[i]],{i,1,Length[Y8]}])/.{\[ExponentialE]^
  Cgf\[Rule]mgf1});ORLI={};
For[i=1,i<TRUNC+1,
  If[i\[Equal]1,AppendTo[ORLI,Compositions[i,Nodes]],
    AppendTo[ORLI,Join[ORLI[[i-1]],Compositions[i,Nodes]]];i++];
orderList1=Last[ORLI];ORLI={};
relationsmod=

MomCumConvert[#,ForMomentQ\[Rule]"Y",CenteredQ\[Rule]"N",

MomentSymbol\[Rule]m,CumulantSymbol\[Rule]K]&/@orderList1;
relations=relationsmod/.{K[r_]\[Rule]K[r][t]};
momcumrule=relations/.{Equal\[Rule]Rule};AO=AN^AH;
T1=Table[Times@@AO/.Thread[AH->orderList1[[i]]],{i,1,Length[orderList1]}];
butt=Table[Thread[AN-
>Sign[orderList1[[i]]],{i,1,Length[orderList1]}];
Y12={};
butt2=
  Table[Table[
If[Sign[orderList1[[j,i]]]\[Equal]1,a,butt[[j,i]]],{i,1,

```

```

Length[orderList1[[1]]]],{j,1,Length[orderList1]}};

For[i=1,i<Length[butt2]+1,AppendTo[Y12,DeleteCases[butt2[[i
]],a]];i++];
  {LHSpde,Y12,T1,Y11,momcumrule}
]

(*This function does the moment matching operation*)
EquateCoefficients[F_,B_,TRUNC_]:=
Module[{LLL,BF,LHSpde,Y12,T1,Y11,momcumrule},

LLL=EQUATE[F,B,TRUNC];LHSpde=LLL[[1]];Y12=LLL[[2]];T1=LLL[[
3]];
Y11=LLL[[4]];momcumrule=LLL[[5]];
BF=Flatten[
  Table[Coefficient[LHSpde/.Y12[[i]],T1[[i]]]\[Equal]
    Coefficient[Y11/.Y12[[i]],T1[[i]]],{i,1,
    Length[T1]}/.momcumrule]
]

(*This function set initail conditions if any and produces
the Equations for \
NDSolve thus this will allow the building of all necesarry
function in order \
to solve the PDEs numerically*)
InitialConditions[F_,B_,TRUNC_,NodeID_,Initial_]:=
Module[{ORLI,orderList1,BE,
Nodes,BE1,BE2,neweqns,neweqmod,BG,BH,BI,BJ,BK,
BL,BM,BF},
Nodes=Length[B[[1]]];
ORLI={};
For[i=1,i<TRUNC+1,
  If[i\[Equal]1,AppendTo[ORLI,Compositions[i,Nodes]],
    AppendTo[ORLI,Join[ORLI[[i-
1]],Compositions[i,Nodes]]]];i++];

orderList1=Last[ORLI];Clear[ORLI];BE=MapThread[K,Transpose[
orderList1]];

BE1=BE/.{K[y_]\[Rule]K[y]'[t]};BE2=BE/.{K[y_]\[Rule]K[y][
0]\[Equal]0};
BF=EquateCoefficients[F,B,TRUNC];neweqns=Solve[BF,BE1];
neweqmod=neweqns/.{Rule\[Rule]Equal};

If[Length[NodeID]\[GreaterEqual]1&&Length[Initial]\[Greater
Equal]1,BG={};

```



```

For[j=1,j<Length[Initial]+1,
  For[i=1,i<Length[orderList1]+1,

If[NodeID[[j]]\[Equal]orderList1[[i]],AppendTo[BG,i]];i++;
j++];

BH=MapThread[K,Transpose[NodeID]];BI=BH/.{K[n__]\[Rule]K[n]
[0]};BJ={};

For[i=1,i<Length[Initial]+1,AppendTo[BJ,BI[[i]]\[Equal]Init
ial[[i]]];

i++;BK={};AppendTo[BK,ReplacePart[BE2,BJ[[1]],BG[[1]]]];
  If[Length[Initial]>1,
    For[i=1,i<Length[Initial]+1,
      If[i\[NotEqual]1,
        AppendTo[BK,ReplacePart[BK[[i-
1]],BJ[[i]],BG[[i]]]];i++];
      BL=Last[BK];BM=Join[BF,BL],BM=Join[BF,BE2];];
    {BM,BE}
  ]
(*This function obtains the numerical evaluated functions
and return \
interpolating functions*)
NumericalSolution[BM_,BE_,TimeAxis_]:=

Module[{rs},rs=NDSolve[BM,BE,{t,0,TimeAxis},MaxSteps\[Rule]
10000]]
(*This function calls all other functions as well as it
runs all plotting *)
MomentNeglect[F_,B_,TRUNC_,NodeID_,Initial_,TimeAxis_,PlotF
uncs_,RangeList_]:=
  Module[{Sol,INT ,BM,BE},

INT=InitialConditions[F,B,TRUNC,NodeID,Initial];BM=INT[[1]]
;BE=INT[[2]];
  Sol=NumericalSolution[BM,BE,TimeAxis];
  For[i=1,i<Length[PlotFuncs]+1,
    If[Length[RangeList]>=1,
      NotebookWrite[NotebookCreate[],
        Cell[GraphicsData["PostScript",
          DisplayString[
Plot[Evaluate[{Extract[PlotFuncs,i]}/.Sol],{t,0,TimeAxis},
          PlotRange\[Rule]Extract[RangeList,i],
          AxesLabel\[Rule]{t,Extract[PlotFuncs,i]},

```

```

DisplayFunction\[Rule]Identity]], "Graphics"]]],
    NotebookWrite[NotebookCreate[],
        Cell[GraphicsData["PostScript",
            DisplayString[
                Plot[Evaluate[{Extract[PlotFuncs, i]}/.Sol], {t, 0, TimeAxis},
                    PlotRange\[Rule]All,
                    AxesLabel\[Rule]{t, Extract[PlotFuncs, i]},
                DisplayFunction\[Rule]Identity]], "Graphics"]]]]; i++;
    ]

```

APPENDIX B
MCP USERS MANUAL

MCP Users Manual

Reference Manual for the Moment Closure Program

© Timothy I. Matis and Amara Nance, Department of Industrial Engineering and Center for Stochastic Modeling, New Mexico State University. This work was partially supported by grant #F49620-03-1-0310 from the Air Force Office of Scientific Research.

Table of Contents

Table of Contents.....	21
1. Introduction.....	22
2. Before You Start	22
3. Entering a Stochastic System.....	22
3.1. Entering the Intensity Functions	23
3.1.1. Systems with Unit Changes	23
3.1.2. Systems with Bulk Changes	24
3.2. Defining the Truncation Level	24
3.3. Defining the Initial Conditions.....	24
3.3.1. All Cumulants Set to Zero	24
3.3.2. One Non-Zero Cumulant	25
3.3.3. Multiple Non-Zero Cumulants.....	25
3.4. Defining the Output Plots.....	25
4. Running the MCP Program	27
5. Limitations	27
6. Contact Information.....	27

1. Introduction

The Moment Closure Program (MCP) is a Mathematica® package that estimates the cumulants (moments) of a non-linear stochastic system over the transient period. The program does not assume a particular parametric state-distribution for the system apriori, which results in the simple truncation, i.e. equating to zero, of all non-estimated cumulants. This program was originally conceived by Dr. Timothy Matis in 1998 and was refined to its present form by Ivan Guardiola and Karl Adams during the 2003 and 2004 academic years. The project was sponsored by grant #F49620-03-1-0310 from the Air Force Office of Scientific Research, whose support made this work possible.

2. Before You Start

Before using the MCP program, place the file "MOMCUM.m" and "MCP.m" in the folder where the Mathematica program and kernel are located. This is typically in the directory *C:\Program Files\Wolfram Research\Mathematica\5.0* for PC versions of Mathematica. The package "MOMCUM.m" was authored by Dr. Qui Zheng, presently with the Department of Bio-Statistics at Texas A&M University, and is necessary for converting moments to cumulants as part of the internal calculations of the "MCP.m" package.

3. Entering a Stochastic System

The first step in entering a stochastic system into Mathematica© is to read in the MCP package. This is accomplished by typing the following command into the first line of a notebook.

```
<<MCP.m
```

On the second line, a function that calls information in this package is entered. The arguments of this function describe all necessary information about the network. This function is given below, and the arguments are described in the following subsections.

MomentNeglect[F,B,TRUNC,NodeID,Initial,TimeAxis,PlotFuncs,RangeList]

3.1. Entering the Intensity Functions

Instantaneous changes in the state of the system in $(t, t+\Delta t)$ and their corresponding intensity functions are entered into the lists B and F respectively. It follows that the lists B and F must be of the same length and that the elements of B and F correspond by position. Note that B is entered as a list of lists and F is entered as a list of functions.

The variables of the intensity functions must be entered as a subscripted letters (note: letters without a subscript will not work properly). As an example, the variable corresponding to the state of the first node should be entered as x_1 . All other elements of the intensity function should be entered in numeric form. The following two examples consider systems that are subject to 1) unit changes and 2) bulk changes in $(t, t+\Delta t)$.

3.1.1. Systems with Unit Changes

Consider a 2-node system with instantaneous unit changes in the state of the system. In particular, arrivals to the first node occur at a rate 3, departures from the first node and the subsequent arrivals to the second node occur according to the rate function $4 x_1^2$, and departures from the second node occur according to the rate function $5 x_2^3$. To specify this system, the following lists would be defined for B and F.

B={{1,0},{-1,1},{0,-1}}

F={3, 4 x_1^2 , 5 x_2^3 }

3.1.2. Systems with Bulk Changes

Consider a single node system with bulk arrivals and unit departures. In particular, arrivals to the first node occur 3 at a time at a rate 5 and departures occur according to the rate function $4 x_1^2$. To specify this system, the following lists would be defined for B and F.

$$B=\{\{2\},\{-1\}\}$$

$$F=\{5, 4 x_1^2\}$$

3.2. Defining the Truncation Level

The first element defined by the user is the truncation level of the cumulants. This value may be set arbitrarily high within the limits of available memory, yet is typically 2,3, or 4 as this is common for many moment closure problems. An example of the truncation level set to 3 is given below.

$$TRUNC=3$$

3.3. Defining the Initial Conditions

Next, the initial conditions are specified. There are three conditions that may exist for the system, 1) all cumulants set to zero, 2) one non-zero cumulant, and 3) more than one non-zero cumulant.

3.3.1. All Cumulants Set to Zero

The default initial condition of the program sets all cumulants to zero at time zero. Hence, leave the lists "NodeID" and "Initial" empty as shown below.

$$NodeID:=\{\}$$

$$Initial:=\{\}$$

3.3.2. One Non-Zero Cumulant

If the initial conditions consist of one non-zero cumulant, identify that cumulant in "NodeID" and enter the non-zero value in "Initial". Note that "NodeID" is entered as a list of lists and "Initial" is entered as a list of numbers. As an example, suppose at time = 0 there are five items in node three of a five node system and that all other nodes are known to be empty. To enter this initial condition, specify "NodeID" in the form of a list using 1 in the third position to indicate the first cumulant of the third node and then specify 5 in the first position of the "Initial" list as shown below.

NodeID:={ {0,0,1,0,0} }

Initial:={5}

3.3.3. Multiple Non-Zero Cumulants

The procedure for entering initial conditions for multiple non-zero cumulants is a simple extension of that for one-cumulant only. The non-zero cumulants are identified as a list in "NodeID" and their values are entered in the corresponding position in "Initial". As an example, suppose at time = 0 it is known that there are 10 items in node three and that the expected number of items in node 4 is 12 with a variance of 5. These initial conditions are entered as shown below.

NodeID:={ {0,0,1,0,0}, {0,0,0,1,0}, {0,0,0,2,0} }

Initial:={10,12,5}

3.4. Defining the Output Plots

The variables that control the output plots of the network are "PlotFuncs", "TimeAxis", and "RangeList". The cumulants that the user would like to view are entered into the list "PlotFuncs" as the elements $K[i,j,\dots][t]$, where i,j,\dots are the non-negative integers corresponding to this set of cumulants. Note that any desired marginal

and cross cumulants up to the order of truncation may be specified in this list. As a reminder, the first order marginal cumulants correspond directly to expectation, the second to the variance, and the third to the skewness. Likewise the second order cross cumulants correspond directly to the covariance between the respective nodes. As an example, consider a fully defined 5-node stochastic network and assume our interest lies only in the expectation and variance of the first node. The specification of these output plots would be entered in the list “**PlotFuncs**” as shown below.

PlotFuncs={K[2,0,0,0,0][t],K[1,0,0,0,0][t]};

The range of the x and y axis of these plots are specified through “**TimeAxis**” and “**RangeList**” respectively. In particular, “**TimeAxis**” controls the range of the independent time variable on the x-axis and “**RangeList**” specifies the range the cumulant on the y-axis. “**TimeAxis**” does not have a default value and must be specified by the user for the program to function properly. “**TimeAxis**” is entered as a single real number that denotes the end point of the interval [0, “**TimeAxis**”]. “**RangeList**” defaults to an interval which is large enough to show the entire value of the cumulant on the y-axis. Often “**RangeList**” is left blank for the first run for the user to visual the entire graph. “**RangeList**”, is modified by entering embedded lists of the form {lower endpt of y, upper endpt of y} that correspond by position to those plots specified in “**PlotFuncs**”. Hence, the lists “**PlotFuncs**” and “**RangeList**” must be of the same length. As an example, consider the two cumulants specified in “**PlotFuncs**” in the previous example. Suppose the user would like to solve for these cumulants from time $t \in [0,50]$ and plot $K[2,0,0,0,0][t]$ on the interval {0,25} and plot $K[1,0,0,0,0][t]$ on the

interval {5,50}. The values of “TimeAxis” and “RangeList” would be entered as shown below.

TimeAxis=50;

RangeList={{0,25},{5,50}};

4. Running the MCP Program

The MCP program may be run by clicking on the “Kernel” menu, then “Evaluation”, then “Evaluate Notebook”. This will generate the specified output graphs labeled with the corresponding cumulant in their own window. For example, the graph of the first cumulant of the first node will have the label “K[1,0,0,0,0,0][t]” and will open in the window “Untitled_1”.

5. Limitations

The program, as written, has a limit of twenty six nodes. If the system under consideration contains more than twenty six nodes, the number of variables in a list that is embedded in the internal calculations section of the program must be increased. To do this, find the list “AG” in the “MCP.m” package and add variables to this list.

6. Contact Information

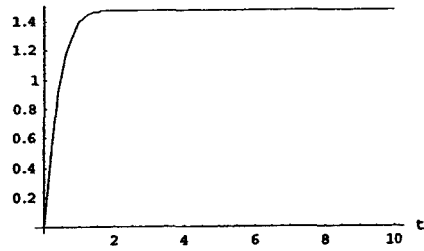
For further information about the MCP program, please contact Dr. Timothy I. Matis at tmatis@nmsu.edu.

APPENDIX C
SAMPLE IMPLEMENTATION OF MCP.m

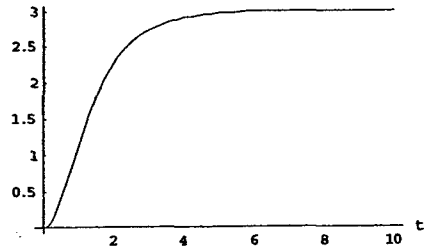
<< MCP.m

MomentNeglect[{3, x_1^2 , x_2 }, {{1, 0}, {-1, 1}, {0, -1}},
3, {}, {}, 10, {K[1, 0][t], K[0, 1][t]}, {All, All}]

K[1, 0][t]



K[0, 1][t]



APPENDIX D
TRANSIENT QUEUEING NETWORK ANALYSIS OF SORTIE GENERATION

Transient Queueing Network Analysis of Aircraft Sortie Generation¹

Timothy I. Matis²

Department of Industrial Engineering, MSC 4230

New Mexico State University

P.O. Box 30001

Las Cruces, NM 88003-8001

Phone: (505) 646-2957; Fax: (505) 646-2976; Email: tmatis@nmsu.edu

and

Jeffrey P. Kharoufeh

Department of Operational Sciences

Air Force Institute of Technology

AFIT/ENS, Building 640

2950 Hobson Way

Wright Patterson AFB, OH 45433-7765

Phone: (937) 255-6565 x 4336; Fax: (937) 656-4943; Email: Jeffrey.Kharoufeh@afit.edu

Abstract

This paper develops a procedure for the transient analysis of an aircraft sortie generation process that is modelled as a closed network of state-dependent queues. The procedure uses the cumulant function method for queueing networks to solve for key time-variant performance measures such as the mean workload at each station and the sortie generation rate. Moreover, the model incorporates a phase-type (PH) service time distribution for maintenance activities and accounts for aircraft blocking at this node. We demonstrate the implementation of the transient technique by means of a notional example.

¹The views expressed in this paper are those of the authors and do not reflect the official policy or position of the United States Air Force, Department of Defense, or the U.S. Government.

²Author supported in part by a grant from the Air Force Office of Scientific Research (F49620-03-1-0310). Author to whom correspondence should be sent.

1 Introduction

In a highly volatile world environment, military decision makers are currently faced with the daunting task of accurately assessing the ability of their forces to carry out critical missions in an efficient and expedient manner. The successful execution of such missions, particularly those involving military aircraft, hinges upon the availability of resources such as personnel, aircraft, munitions, and maintenance facilities. Assessing the operational readiness of a given air base is therefore of paramount importance to military decision makers.

The concept of operational readiness can refer to a number of performance measures within this context. One important measure is that of resource availability which refers to the proportion of time the air base is able to provide all necessary resources and personnel to perform a mission. A few examples of these resources include diagnostic equipment, tools, replacement aircraft components, and physical hangar space necessary to perform maintenance activities. Ultimately, decision makers are interested in the number of successful missions flown over a critical period of time. This measure is often referred to as the aircraft sortie generation rate. It is obvious that the sortie generation rate is highly dependent on the flow of ground operations. Perhaps the most critical portion of the overall sortie generation process is the maintenance activity. This is due to the fact that distinct aircraft may have vastly differing maintenance requirements upon sortie completion. For this reason, it is crucial to assess such measures as the current workload at the maintenance station(s) as well as resource availability. However, these measures are not necessarily time invariant, particularly in wartime scenarios in which prevailing theater-level dynamics may govern ground operations. The time-variant behavior of these measures ultimately impacts the ability of an airfield to fly aircraft sorties.

Owing to the inherently complex interactions between resources required for the sortie generation process, analysts have typically employed computer simulation techniques for the purpose of evaluating operational readiness. In the United States Air Force, for instance, some typical models that have been employed are the Logistics Composite Model (LCOM) [3] and the Sortie Generation Model (SGM) [1]. Though such simulations allow analysts to assess the utilization of resources (and other performance metrics), the implementation of such models can be cumbersome due to extensive data input requirements and long run times for a single replication. These problems are exacerbated in a real-time setting when decision makers need reasonable answers in an expedient manner.

In order to address the shortcomings of simulation models of air base operations, some authors have proposed analytical models to measure some basic aggregate features that can be used to quickly and adequately answer important questions regarding operational readiness. More specifically, Dietz and Jenkins [2] provided a mathematical framework to address the problem of modelling the theater-level dynamics of the aircraft sortie generation process as a closed queueing network. In that work, the authors presented a steady-state, mean value analysis (MVA) for several important performance measures involved in the aircraft sortie generation process. The key innovation in their model was the incorporation of a single, fork-join node in the queueing network that enables the analytical modelling of concurrent maintenance activities subsequent to sortie completion. This approach to the problem is significant for several reasons. First, it allows for an aggregation of many complexities into single- or multi-server queueing stations. Second, it provides an analytical framework upon which to build models of higher resolution if needed, and third, it provides fast numerical results for decision makers who require a "snapshot" of their current operational capability by avoiding time-consuming simulation replications. Hackman and Dietz [6] extended the preliminary work of [2] by allowing the service times at each node of the network (i.e., at each stage of the sortie generation process) to be arbitrarily distributed rather than exponentially distributed.

Though these two papers provide a framework upon which the sortie generation process may be analyzed, the work does suffer an important shortcoming. Both works provide a steady-state, mean value analysis (MVA) of the workload at each node and the sortie generation rate as opposed to a more realistic transient analysis. Although the steady-state analysis allows for mathematical tractability of the model, it fails to incorporate the realistic, time-variant behavior of the important measures of operational readiness. Additionally, the queueing network models developed in these papers do not account for the blocking of aircraft that occurs at the maintenance node due to limited hangar space. Hence, the primary objective of our work is to extend that of Dietz and Jenkins [2] and Hackman and Dietz [6] by explicitly incorporating the time dependence of queueing performance measures for a more accurate assessment of operational readiness by using a new analytical technique for the transient analysis of queueing networks.

The main contributions of this work can be summarized as follows. We provide a transient analysis for a closed queueing network model of the sortie generation process. The primary measure of operational readiness is the time-variant sortie generation rate, though

we also consider the workload (or congestion level) of the system measured by the expected number of aircraft present at each station at a given point in time. To that end, we formulate a phase-type approximation for the distribution of aircraft holding time at the fork-join repair node, and adapt and employ the cumulant function method previously applied to queueing networks by Matis and Feldman [9]. Our approach to the problem allows us to compute the first moment of the aforementioned measures as explicit functions of time.

The remainder of the paper is organized in the following manner. Section 2 reviews the important features of the steady-state model of [2]. In section 3, we present our modified queueing network model of the aircraft sortie generation process. Section 4 discusses the cumulant-based, transient analysis of the queueing network while section 5 provides a numerical example demonstrating the implementation of the procedure. Finally, we give some concluding remarks in section 6.

2 Queueing Network Model

Dietz and Jenkins [2] were apparently the first to present a formal mathematical model of the sortie generation process. Before describing our transient analysis and extensions of their model, we provide a brief review of the latter. There are six activities that can be identified in the process of flying sorties from a given air base. In the queueing network framework of [2], each activity is modelled as an individual queueing station. The flow entities of the network are a fixed number of aircraft (N) that pass through the six nodes (stations) according to a stochastic routing matrix $P := [p_{ij}]$ where p_{ij} denotes the stationary probability that an aircraft completing activity i proceeds next to activity j . The network is assumed to be closed in that the N aircraft never leave the system, nor do additional aircraft arrive to the system. The closed queueing network model consists of the following nodes: pre-flight, sortie, troubleshoot, a fork-join maintenance node, turnaround, and munitions upload. The fork-join node consists of five substations representing five critical systems of an aircraft that may or may not require maintenance subsequent to sortie completion and the troubleshooting activity. Each station is assumed to have an exponentially distributed service time. Figure 1 gives a graphical depiction of the flow of aircraft through this network.

The closed queueing network model was analyzed using a mean value analysis (MVA) heuristic developed by Rao and Suri [11] to accommodate the nuance of a fork-join node and enhanced by Jenkins [7] to handle fork-join nodes with probabilistic branching. While the

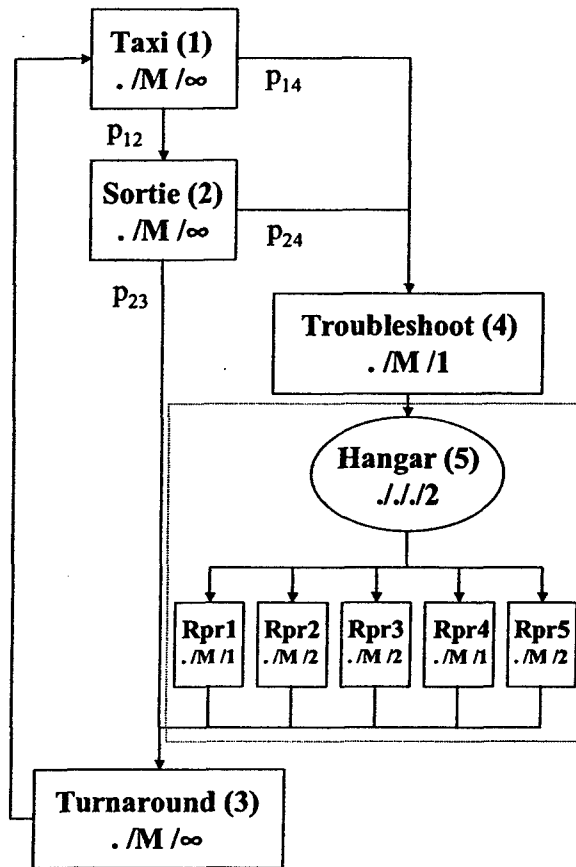


Figure 1: Queueing network model of sortie generation process.

MVA produces exact results for product-form networks, the heuristic MVA procedure provides only approximate performance measure values for any closed network with more than one customer in the system. Using this approach, the primary (steady-state) performance measures computed in [2] were: i) the mean number of aircraft at each station (workload), ii) the throughput at each station, and iii) the overall throughput of the network, which directly corresponds to the time-invariant sortie generation rate. These results are useful due to their mathematical tractability and ease of implementation; however, they do not account for the inherently time-variant behavior of the station (or system) workload and the sortie generation rate. Moreover, the model of [2] ignores the effects of blocking by assuming infinite capacity queues at each station; however, limited hangar space is a reality at most air bases causing aircraft to be blocked at the troubleshoot node of the network.

In the following section, we present a modified version of the basic model of Dietz

and Jenkins [2] in order to consider the transient (time-dependent) behavior of the expected workload in the system and the sortie generation rate. In the subsequent section, we describe the formal procedure for analyzing the model in the transient regime.

3 Modified Queueing Network Model

The first significant difference in our model is the characterization of the holding time in the maintenance hangar as a phase-type (PH) distribution. PH distributions are extremely useful when modeling the distributions of nonnegative random variables. Figure 2 gives a graphical depiction of our modified queueing network model.

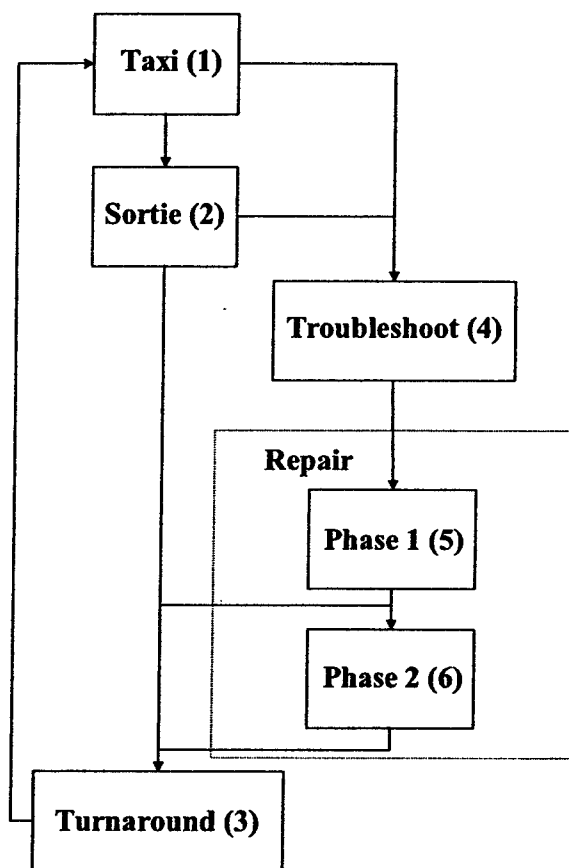


Figure 2: Sortie generation model with PH-distributed repair times.

It is important to note the distinction between the models of Figures 1 and 2. In Figure 2, it is compulsory to add node 6 to the maintenance node (node 5 of Figure 1) in order to implement our two-phase holding time distribution.

For our modified model, we adopt the notation in [2]. Referring to Figure 1, let s_i denote the mean service time at node i , and let r_i denote the number of servers at node i , for $i = 1, 2, 3, 4$. Owing to the fact that service rates are state dependent, whenever n customers are present at node i , the state-dependent service rate, $\mu_i(n)$, is given by

$$\mu_i(n) = \min\{n/s_i, r_i/s_i\}, \quad i = 1, 2, 3, 4. \quad (1)$$

With regard to node 5 of Figure 1, the fork-join repair node, we define $s_{5,k}$ as the mean service time at repair station k , $r_{5,k}$ denotes the number of servers at repair station k , and $q_{5,k}$ is the probability that repair activity k is required by an arriving aircraft, $k = 1, 2, 3, 4, 5$. The state-dependent service rates for the maintenance activities are thus

$$\mu_{5,k}(n) = \min\{n/s_{5,k}, r_{5,k}/s_{5,k}\}, \quad k = 1, 2, 3, 4, 5. \quad (2)$$

The service rates of Equation (2) correspond to the rate parameters of the associated exponential distributions at each of the five repair stations of node 5. For our particular queueing network model, the parameter values are summarized in Table 1.

Table 1: Model parameter values for sortie generation queueing network.

Node Index	Mean Service Time	Repair Probability	Number of Servers
1	$s_1 = 0.25$		$r_1 = \infty$
2	$s_2 = 2.00$		$r_2 = \infty$
3	$s_3 = 1.25$		$r_3 = \infty$
4	$s_4 = 0.50$		$r_4 = 1$
5,1	$s_{5,1} = 2.20$	$q_{5,1} = 0.17$	$r_{5,1} = 1$
5,2	$s_{5,2} = 2.27$	$q_{5,2} = 0.39$	$r_{5,2} = 2$
5,3	$s_{5,3} = 2.37$	$q_{5,3} = 0.21$	$r_{5,3} = 2$
5,4	$s_{5,4} = 1.50$	$q_{5,4} = 0.27$	$r_{5,4} = 1$
5,5	$s_{5,5} = 1.19$	$q_{5,5} = 0.46$	$r_{5,5} = 2$

It should be noted that the activity labelled “munitions upload” in [2] is contained in the “turnaround” activity in this model so that the total mean service time at the turnaround queue is 1.25 time units.

We examine the operational readiness of a single air base that services N aircraft with a maintenance hangar capacity of 2 planes (i.e., we relax the assumption that the maintenance hangar has infinite capacity). An airplane undergoing service will occupy a hangar space until all required service activities have been completed. The troubleshooting activities of node 4 will be halted when the hangar is full and will resume only when a departing

aircraft frees capacity in the subsequent repair node. The repair activities of node 5 are performed concurrently and assumed to be mutually independent. In the following subsection, we describe the means by which the original fork-join construction of the repair node is used to provide a phase-type representation of the maintenance holding time distribution. The parameters of the phase-type distribution will ultimately be used to describe the stochastic evolution of the system, thereby allowing for our transient analysis procedure.

3.1 PH Distribution for Repair Holding Times

The distribution of aircraft holding time at the fork-join repair node shall be represented by a continuous three-parameter, two-phase, state-dependent distribution. We first briefly review PH distributions which are described in detail in the pioneering book by Neuts [10]. Consider a Markov process on a finite state space $\mathcal{E} := \{1, 2, \dots, u+1\}$ such the state j is transient for $1 \leq j \leq u$, and state $u+1$ is the absorbing state. The infinitesimal generator matrix Q of this process may be partitioned as

$$Q = \begin{bmatrix} \mathbf{G} & \mathbf{G}^0 \\ \mathbf{0} & 0 \end{bmatrix} \quad (3)$$

where the elements of the $u \times u$ matrix \mathbf{G} are such that $G_{ii} < 0$ and $G_{ij} \geq 0, i \neq j$. Moreover,

$$\mathbf{G}\mathbf{e} + \mathbf{G}^0 = \mathbf{0}$$

where \mathbf{e} is a column vector of ones. The initial distribution of the Markov process is given by the row vector $\alpha' := (\underline{\alpha}, \alpha_{u+1})$ where $\underline{\alpha}$ is a row vector, α_{u+1} is the probability that the process begins in state $u+1$, and

$$\underline{\alpha}\mathbf{e} + \alpha_{u+1} = 1.$$

A probability distribution F for a nonnegative random variable is said to be a PH distribution if and only if it is the distribution of the random time until absorption of the aforementioned Markov process. In such case, the distribution is said to have representation $(\underline{\alpha}, \mathbf{G})$.

The representation of repair holding times necessarily incorporates the state dependence of service rates for individual repair activities. Following the notational convention of Neuts [10], the PH distribution is denoted by the ordered pair $(\underline{\alpha}, \mathbf{G}(n))$ where $\mathbf{G}(n)$ is the matrix of state-dependent transition rates. In this work, the holding time distribution at the repair node has the representation

$$(\underline{\alpha}, \mathbf{G}(n)) = \left((1, 0), \begin{bmatrix} -(\nu_1(n) + \nu_2(n)) & \nu_1(n) \\ 0 & -\nu_3(n) \end{bmatrix} \right) \quad (4)$$

where $\nu_i(n)$, $i = 1, 2, 3$, denote the unknown parameters of the phase-type distribution. In order to describe the stochastic evolution of this system, our aim is to determine these unknown parameters by matching moments.

Referring to Figure 1, let $T_{5,k}$, $k \in \{1, \dots, 5\}$, be an exponentially distributed random variable representing the aircraft holding time at repair node k , and let $N_5(t) \in \{0, 1, 2\}$ denote the number of aircraft in the repair hangar of node 5 at time t . The moments $E[T_{5,k}^j | N_5(t) = n]$, $j = 1, 2, 3$, may be calculated for repair activity k using the exponential assumption of individual repair times by

$$E[T_{5,k}^j | N_5(t) = n] = \int_0^\infty t^j \mu_{5,k}(n) e^{-\mu_{5,k}(n)t} dt.$$

Let $\Omega = \{\emptyset, \{1\}, \dots, \{1, 2, 3, 4, 5\}\}$ be the set of all possible repair activity combinations for an aircraft. From the independence of the repair activities, the probability that the set $\omega \in \Omega$ is required by an arriving aircraft, π_ω , is

$$\pi_\omega = \prod_{k \in \omega} q_{ik} \prod_{k \notin \omega} (1 - q_{ik}). \quad (5)$$

Denote by a continuous random variable, T_5 , the total time spent by an aircraft in the hangar at node 5 until all required repair activities have been completed. The conditional moments $E[T_5^j | N_5(t) = n]$, $j = 1, 2, 3$, may be calculated as

$$E[T_5^j | N_5(t) = n] = \sum_{\omega \in \Omega} \pi_\omega E[\max_{k \in \omega} \{T_{5,k}^j\} | N_5(t) = n]. \quad (6)$$

For the queueing network model defined in Table 1, the moments of T_5 are given by

Table 2: Repair time moments.			
n	$E[T_5 N_5(t) = n]$	$E[T_5^2 N_5(t) = n]$	$E[T_5^3 N_5(t) = n]$
0	0	0	0
1	2.07944	9.33339	61.6057
2	1.82659	7.63503	48.3688

Suppose X is a nonnegative random variable with PH representation $(\underline{\alpha}, \mathbf{G})$. Then it is well known (cf. Kao [4]) that the j^{th} moment of X can be obtained by

$$E[X^j] = (-1)^j j! \underline{\alpha} \mathbf{G}^{-j} \mathbf{e}, \quad j \geq 1. \quad (7)$$

For $j = 1, 2, 3$ and each $n \in \{0, 1, 2\}$, the moments of the phase-type distribution defined in Equation (4) are calculated and matched to those given in Table 2 using Eq. (7) by

$$E[T_5^j | N_5(t) = n] = (-1)^j j! (1, 0) \begin{bmatrix} -(\nu_1(n) + \nu_2(n)) & \nu_1(n) \\ 0 & -\nu_3(n) \end{bmatrix}^{-j} \begin{pmatrix} 1 \\ 1 \end{pmatrix}. \quad (8)$$

This operation generates three sets of three algebraic equations whose simultaneous solution yields estimates for the unknown parameters $\nu_i(n)$, $i = 1, 2, 3$, of the phase-type distribution. For our defined queueing network model, these parameter estimates are listed in Table 3.

Table 3: Parameters of the PH distribution.

n	$\nu_1(n)$	$\nu_2(n)$	$\nu_3(n)$
0	0	0	0
1	12.2582	1.4874	0.42102
2	5.1942	1.36185	0.47136

The phase-type representation of the fork-join nodes is incorporated into the model of sortie generation depicted in Figure 1 yielding the model representation displayed in Figure 2. In what follows, we discuss the stochastic evolution of this closed queueing network before presenting the transient analysis procedure of section 4

3.2 Stochastic Evolution of the System

The evolution of this stochastic, time-variant system is described as follows. Let $X_i(t)$ denote the number of aircraft at station i at time $t > 0$ and let the multivariate stochastic process $\{X_i(t) : t \geq 0, i = 1, 2, \dots, 6\}$ describe the state of the network at time t . The state space E_i of $X_i(t)$ is given by $E_i = \{0, 1, 2, \dots, N\}$, for $1 \leq i \leq 6$. We will henceforth denote this vector-valued, Markov process by $\{\mathbf{X}(t) : t \geq 0\}$ where $\mathbf{X}(t) = (X_1(t), \dots, X_6(t))$. In a small interval of time $(t, t + \delta t)$, we note that, for each node of the queueing network, the change of state may decrease by one aircraft, increase by one aircraft, or remain the same. We describe this collection of all possible state changes by the set

$$\mathcal{B} = \{(-1, 1, 0, 0, 0, 0), (-1, 0, 0, 1, 0, 0), (0, -1, 1, 0, 0, 0), (0, -1, 0, 1, 0, 0), (0, 0, -1, 0, 0, 1), \\ (0, 0, 0, -1, 1, 0), (0, 0, 0, 0, -1, 1), (1, 0, 0, 0, -1, 0), (1, 0, 0, 0, 0, -1)\}. \quad (9)$$

The intensity functions corresponding to the elements of this set will be denoted as

$$f_{(b_1, \dots, b_6)}(x_1, \dots, x_6)$$

for $x_i \in E_i$. Combining information from Tables 1 and 3, the functions corresponding to (9) are specified in Table 4 where $I_{[l,u]}(x)$ is a 0,1 indicator function on E_i for $x \in [l, u]$. These defined intensity functions will be represented as finite polynomial functions of the form

$$f_{b_1, \dots, b_6}(x_1, \dots, x_6) = \phi(b_1, \dots, b_6) h_{b_1, \dots, b_6}(x_1, \dots, x_6), \quad (10)$$

where $\phi(b_1, \dots, b_6)$ is a constant and $h_{b_1, \dots, b_6}(x_1, \dots, x_6)$ is a polynomial function, for the purpose of subsequent cumulant-based mathematical operations.

Table 4: Intensity functions for the aircraft sortie model.

$(b_1, \dots, b_6) \in \mathcal{B}$	$f_{b_1, \dots, b_6}(x_1, \dots, x_6)$
$(-1, 1, 0, 0, 0, 0)$	$p_{12}(x_1/s_1) = 4.0p_{12}x_1$
$(-1, 0, 0, 1, 0, 0)$	$p_{14}(x_1/s_1) = 4.0p_{14}x_1$
$(0, -1, 1, 0, 0, 0)$	$p_{23}(x_2/s_2) = 0.25p_{23}x_2$
$(0, -1, 0, 1, 0, 0)$	$p_{24}(x_2/s_2) = 0.25p_{24}x_2$
$(1, 0, -1, 0, 0, 0)$	$x_3/s_3 = 0.80x_3$
$(0, 0, 0, -1, 1, 0)$	$(x_4/s_4)I_{[0,1]}(x_5 + x_6) \approx 2x_4 (1 + 0.5(x_5 + x_6) - 0.5(x_5 + x_6)^2)$
$(0, 0, 0, 0, -1, 1)$	$\nu_1(0)I_{[0,0]}(x_5) + \nu_1(1)I_{[1,1]}(x_5)I_{[0,0]}(x_6) + \nu_1(2)(I_{[2,2]}(x_5)I_{[0,0]}(x_6) + I_{[1,1]}(x_5)I_{[1,1]}(x_6))$ $= 21.9193x_5 - 9.66108x_5^2 - 7.06402x_5x_6$
$(1, 0, 0, 0, -1, 0)$	$\nu_2(0)I_{[0,0]}(x_5) + \nu_2(1)I_{[1,1]}(x_5)I_{[0,0]}(x_6) + \nu_2(2)(I_{[2,2]}(x_5)I_{[0,0]}(x_6) + I_{[1,1]}(x_5)I_{[1,1]}(x_6))$ $= 2.29388x_5 - 0.806475x_5^2 - .12555x_5x_6$
$(1, 0, 0, 0, 0, -1)$	$\nu_3(0)I_{[0,0]}(x_6) + \nu_3(1)I_{[1,1]}(x_6)I_{[0,0]}(x_5) + \nu_3(2)(I_{[2,2]}(x_6)I_{[0,0]}(x_5) + I_{[1,1]}(x_6)I_{[1,1]}(x_5))$ $= 0.605482x_6 - 0.184451x_6^2 + .05034x_6x_5$

The intensity functions of Table 4 depend explicitly on the parameters of the PH distribution $(\nu_i(n), 1 \leq i \leq 3)$. In what follows, we present the means by which to apply cumulant functions for the purpose of performing a transient analysis of the Markov process $\{X(t) : t \geq 0\}$. In particular, our interest is in approximating the time-variant functions $E[X_i(t)]$ for $i = 1, \dots, 6$ as well as the time-variant sortie generation rate.

4 Cumulant-Based Transient Analysis

There are relatively few analytical procedures through which the Markov process $\{X(t) : t \geq 0\}$ may be practically analyzed over the transient period. Many of the existing analytical techniques suffer from either a high degree of mathematical complexity or from computational intractability. As an example, consider the common approach of using Kolmogorov differential equations to obtain the transient state probabilities of $\{X(t) : t \geq 0\}$.

The number of such equations is given by

$$\left(1 + \sum_{i=1}^n c_i\right)^n \quad (11)$$

where n denotes the number of nodes in the network and c_i is the capacity of the i^{th} node. As an example, the previously defined queueing network with $n = 6$ and $c_i = N$ for all i , generates approximately 5.15×10^{10} differential equations when $N = 10$ aircraft and 7.43×10^{14} equations when $N = 50$ aircraft. Hence, the number of Kolmogorov differential equations tends to intractability for even small N .

Alternatively, a cumulant-based approach may be used to approximate the first order cumulants (means) of the multivariate state distribution of $\{\mathbf{X}(t) : t \geq 0\}$ in a much more computationally efficient manner. Specifically, the number of differential equations using these procedures is

$$\left(\frac{1}{n!} \prod_{i=1}^n (i + m)\right) - 1 \quad (12)$$

where m is the level of cumulant truncation. The specification of $m = 2$ assumes that the state distribution is multivariate normal, which is not practical in most cases. It has been previously shown, however, that raising the truncation level to $m = 3$, which introduces a skewness measure, is sufficient for reasonable approximations of the first cumulant of $X_i(t)$. For the defined queueing network $\{\mathbf{X}(t) : t \geq 0\}$ with $n = 6$ and $m = 3$, 83 differential equations will be generated by a cumulant-based approach independent of N . This set of equations is sufficiently small to facilitate an efficient numerical solution.

The use of cumulant-based analysis procedures for a general n -node network will first be discussed, following which the procedure will be applied to the defined closed queueing network $\{\mathbf{X}(t) : t \geq 0\}$ representing the aircraft sortie generation process.

4.1 General Procedural Description

For $\theta_1, \dots, \theta_n, t > 0$ and \mathcal{I}^+ the set of non-negative integers, let $M(\theta_1, \dots, \theta_n, t)$ be a multivariate moment generating function for $\mathbf{X}(t)$ defined as

$$M(\theta_1, \dots, \theta_n, t) = \sum_{a_1, \dots, a_n \in \mathcal{I}^+} \frac{m_{a_1, \dots, a_n}(t) \theta_1^{a_1} \dots \theta_n^{a_n}}{a_1! \dots a_n!} \quad (13)$$

where $m_{a_1, \dots, a_n}(t)$ are the joint moments of $\mathbf{X}(t)$. Likewise, let $K(\theta_1, \dots, \theta_n, t)$ be a multivariate cumulant generating function defined as

$$K(\theta_1, \dots, \theta_n, t) = \sum_{a_1, \dots, a_n \in \mathcal{I}^+} \frac{k_{a_1, \dots, a_n}(t) \theta_1^{a_1} \dots \theta_n^{a_n}}{a_1! \dots a_n!} \quad (14)$$

where $k_{a_1, \dots, a_n}(t)$ are the joint cumulants of $\mathbf{X}(t)$. By definition (Kendall [5]), the generating functions of Eqs. (13) and (14) have the functional relationship

$$M(\theta_1, \dots, \theta_n, t) = e^{K(\theta_1, \dots, \theta_n, t)}, \quad (15)$$

through which the joint moments define the cumulants of $\mathbf{X}(t)$.

The multivariate moment generating function $M(\theta_1, \dots, \theta_n, t)$ and the polynomial intensity functions $f_{b_1, \dots, b_n}(x_1, \dots, x_n)$ of a Markovian network may be related through the partial differential equation

$$\frac{\partial M(\theta_1, \dots, \theta_n, t)}{\partial t} = \sum_{b_1, \dots, b_n} (e^{b_1 \theta_1 + \dots + b_n \theta_n} - 1) f_{b_1, \dots, b_n} \left(\frac{\partial}{\partial \theta_{b_1}}, \dots, \frac{\partial}{\partial \theta_{b_n}} \right) M(\theta_1, \dots, \theta_n, t) \quad (16)$$

where $f_{b_1, \dots, b_n} \left(\frac{\partial}{\partial \theta_{b_1}}, \dots, \frac{\partial}{\partial \theta_{b_n}} \right) M(\theta_1, \dots, \theta_n, t)$ is a partial differential operator that replaces terms of the form x_j^i in the polynomial function f with the i^{th} partial derivative of $M(\theta_1, \dots, \theta_n, t)$ with respect to θ_j . The partial differential equation of Eq. (16) may be solved directly if possible, yet this is often not plausible due to the frequent complexity and non-linearity of the equation.

As an alternative, an m^{th} order truncated cumulant generating function, defined as

$$K^o(\theta_1, \dots, \theta_n, t) = \sum_{a_1, \dots, a_n \in Z(m)} \frac{k_{a_1, \dots, a_n}(t) \theta_1^{a_1} \dots \theta_n^{a_n}}{a_1! \dots a_n!} \quad (17)$$

for $Z(m) = \{(a_1, \dots, a_n) : a_i \in \mathcal{I}^+, \sum_{i=1}^n a_i \leq m\}$, may be used to extract a closed set of ordinary differential equations from this partial differential equation. In particular, Eq. (17) is substituted into Eq. (16) yielding the expression

$$\frac{\partial e^{K^o(\theta_1, \dots, \theta_n, t)}}{\partial t} = \sum_{b_1, \dots, b_n} (e^{b_1 \theta_1 + \dots + b_n \theta_n} - 1) f_{b_1, \dots, b_n} \left(\frac{\partial}{\partial \theta_{b_1}}, \dots, \frac{\partial}{\partial \theta_{b_n}} \right) e^{K^o(\theta_1, \dots, \theta_n, t)}. \quad (18)$$

Expanding all partial derivatives, performing Taylor series expansions, and substituting expanded moment generating function in Eq. (18) generates the expression

$$\begin{aligned} & \sum_{a_1, \dots, a_n \in \mathcal{I}^+} \frac{m_{a_1, \dots, a_n}(t) \theta_1^{a_1} \dots \theta_n^{a_n}}{a_1! \dots a_n!} \cdot \sum_{a_1, \dots, a_n \in Z(m)} \frac{k'_{a_1, \dots, a_n}(t) \theta_1^{a_1} \dots \theta_n^{a_n}}{a_1! \dots a_n!} = \\ & \sum_{b_1, \dots, b_n} \left(\sum_{k=1}^{\infty} \frac{(b_1 \theta_1 + \dots + b_n \theta_n)^k}{k!} \right) \cdot \left(\sum_{a_1, \dots, a_n \in \mathcal{I}^+} \frac{m_{a_1, \dots, a_n}(t) \theta_1^{a_1} \dots \theta_n^{a_n}}{a_1! \dots a_n!} \right)^{j(b_1, \dots, b_n)} \\ & \cdot \sum_i c_{b_1, \dots, b_n}(i) \psi_{b_1, \dots, b_n}^i(\theta_1, \dots, \theta_n), \end{aligned} \quad (19)$$

where $c_{b_1, \dots, b_n}(i)$ is a constant, $j(b_1, \dots, b_n) \in \mathcal{I}^+$, and $\psi_{b_1, \dots, b_n}^i(\theta_1, \dots, \theta_n)$ is a polynomial function of $\theta_1, \dots, \theta_n$ comprised of moments and non-truncated cumulants. Since both sides of Eq. (19) are polynomial expressions of $\theta_1, \dots, \theta_n$, the coefficients of each unique combination of $\{\theta_1^{a_1} \dots \theta_n^{a_n} : c_i \in \mathcal{I}^+, a_1 + \dots + a_n \leq m\}$ on the left and right hand side must equate. Hence, equating these coefficients and expressing the joint moments $m_{a_1, \dots, a_n}(t)$ as functions of the non-truncated joint cumulants, $k_{a_1, \dots, a_n}(t)$, for $\{a_1, \dots, a_n\} \in Z(m)$ forms a closed set of ordinary differential equations whose solution approximates the time-varying, non-truncated cumulants of $\{X(t) : t \geq 0\}$ up to the m^{th} order.

4.2 Analysis of the Sortie Generation Model

In this subsection, we apply the general cumulant-based procedure to our modified queueing network model for the aircraft sortie generation process. Let $K^o(\theta_1, \dots, \theta_6, t)$ be a third-order ($m = 3$), truncated cumulant generating function defined as in Eq. (17) for the sortie queueing network model $\{X(t) : t \geq 0\}$ defined in section 3. Using Eq. (18), the function $K^o(\theta_1, \dots, \theta_6, t)$ is related to the intensity functions defined in Table 4 through the partial differential equation

$$\begin{aligned} \frac{\partial e^{K(\theta_1, \dots, \theta_6, t)}}{\partial t} = & 4.0p_{12}(e^{\theta_2 - \theta_1} - 1) \frac{\partial e^{K(\theta_1, \dots, \theta_6, t)}}{\partial \theta_1} + 4.0p_{14}(e^{\theta_4 - \theta_1} - 1) \frac{\partial e^{K(\theta_1, \dots, \theta_6, t)}}{\partial \theta_1} \\ & + 0.50p_{23}(e^{\theta_3 - \theta_2} - 1) \frac{\partial e^{K(\theta_1, \dots, \theta_6, t)}}{\partial \theta_2} + 0.50p_{24}(e^{\theta_4 - \theta_2} - 1) \frac{\partial e^{K(\theta_1, \dots, \theta_6, t)}}{\partial \theta_2} \\ & + 0.80(e^{\theta_1 - \theta_3} - 1) \frac{\partial e^{K(\theta_1, \dots, \theta_6, t)}}{\partial \theta_3} + 2.0(e^{\theta_5 - \theta_4} - 1) \frac{\partial e^{K(\theta_1, \dots, \theta_6, t)}}{\partial \theta_4} \\ \times \left(1 + 0.50 \left(\frac{\partial e^{K(\theta_1, \dots, \theta_6, t)}}{\partial \theta_5} + \frac{\partial e^{K(\theta_1, \dots, \theta_6, t)}}{\partial \theta_6} \right) - 0.50 \left(\frac{\partial^2 e^{K(\theta_1, \dots, \theta_6, t)}}{\partial \theta_5^2} + \frac{\partial^2 e^{K(\theta_1, \dots, \theta_6, t)}}{\partial \theta_6^2} + 2.0 \frac{\partial^2 e^{K(\theta_1, \dots, \theta_6, t)}}{\partial \theta_5 \partial \theta_6} \right) \right) \\ & + (e^{\theta_6 - \theta_5} - 1) \left(21.919388 \frac{\partial e^{K(\theta_1, \dots, \theta_6, t)}}{\partial \theta_5} - 9.66108 \frac{\partial^2 e^{K(\theta_1, \dots, \theta_6, t)}}{\partial \theta_5^2} - 7.06402 \frac{\partial^2 e^{K(\theta_1, \dots, \theta_6, t)}}{\partial \theta_5 \partial \theta_6} \right) \\ & + (e^{\theta_3 - \theta_5} - 1) \left(2.29388 \frac{\partial e^{K(\theta_1, \dots, \theta_6, t)}}{\partial \theta_5} - 0.806475 \frac{\partial^2 e^{K(\theta_1, \dots, \theta_6, t)}}{\partial \theta_5^2} - 0.12555 \frac{\partial^2 e^{K(\theta_1, \dots, \theta_6, t)}}{\partial \theta_5 \partial \theta_6} \right) \\ & + (e^{\theta_3 - \theta_6} - 1) \left(0.605482 \frac{\partial e^{K(\theta_1, \dots, \theta_6, t)}}{\partial \theta_6} - 0.184451 \frac{\partial^2 e^{K(\theta_1, \dots, \theta_6, t)}}{\partial \theta_6^2} + 0.05034 \frac{\partial^2 e^{K(\theta_1, \dots, \theta_6, t)}}{\partial \theta_5 \partial \theta_6} \right). \quad (20) \end{aligned}$$

Patterned after Eq. (19), the expansion and substitution operations of the previous subsection are performed on Eq. (20) yielding the general polynomial expression

$$\begin{aligned}
& \left(\sum_{a_i \in \mathcal{I}^+} \frac{m_{a_1, \dots, a_6}(t)}{a_1! \dots a_6!} \right) \left(\sum_{a_i \in \mathcal{Z}(3)} \frac{k'_{a_1, \dots, a_6}(t)}{a_1! \dots a_6!} \right) = \\
& 4.0p_{12} \left(\sum_{i=1}^{\infty} \frac{(\theta_2 - \theta_1)^i}{i!} \right) \Psi_{(-1,1,0,0,0,0)}(\theta_1 \dots \theta_6) + 4.0p_{14} \left(\sum_{i=1}^{\infty} \frac{(\theta_4 - \theta_1)^i}{i!} \right) \Psi_{(-1,0,0,1,0,0)}(\theta_1 \dots \theta_6) \\
& + 0.50p_{23} \left(\sum_{i=1}^{\infty} \frac{(\theta_3 - \theta_2)^i}{i!} \right) \Psi_{(0,-1,1,0,0,0)}(\theta_1 \dots \theta_6) + 0.50p_{24} \left(\sum_{i=1}^{\infty} \frac{(\theta_4 - \theta_2)^i}{i!} \right) \Psi_{(0,-1,0,1,0,0)}(\theta_1 \dots \theta_6) \\
& + 0.80 \left(\sum_{i=1}^{\infty} \frac{(\theta_3 - \theta_1)^i}{i!} \right) \Psi_{(1,0,-1,0,0,0)}(\theta_1 \dots \theta_6) \\
& + 2.0 \left(\sum_{i=1}^{\infty} \frac{(\theta_5 - \theta_4)^i}{i!} \right) \Psi_{(0,0,0,-1,1,0)}^{(1)}(\theta_1 \dots \theta_6) \\
& \times \left(1 + 0.50 \left(\Psi_{(0,0,0,-1,1,0)}^{(2)}(\theta_1 \dots \theta_6) \right) - 0.50 \left(\Psi_{(0,0,0,-1,1,0)}^{(3)}(\theta_1 \dots \theta_6) \right) \right) \\
& + \left(\sum_{i=1}^{\infty} \frac{(\theta_6 - \theta_5)^i}{i!} \right) \\
& \times \left(21.9193 \Psi_{(0,0,0,0,-1,1)}^{(1)}(\theta_1 \dots \theta_6) - 9.66108 \Psi_{(0,0,0,0,-1,1)}^{(2)}(\theta_1 \dots \theta_6) - 7.06402 \Psi_{(0,0,0,0,-1,1)}^{(3)}(\theta_1 \dots \theta_6) \right) \\
& + \left(\sum_{i=1}^{\infty} \frac{(\theta_3 - \theta_5)^i}{i!} \right) \\
& \times \left(2.29388 \Psi_{(0,0,1,0,-1,0)}^{(1)}(\theta_1 \dots \theta_6) - 0.806475 \Psi_{(0,0,1,0,-1,0)}^{(2)}(\theta_1 \dots \theta_6) - 0.12555 \Psi_{(0,0,1,0,-1,0)}^{(2)}(\theta_1 \dots \theta_6) \right) \\
& + \left(\sum_{i=1}^{\infty} \frac{(\theta_3 - \theta_6)^i}{i!} \right) \\
& \times \left(0.605482 \Psi_{(0,0,1,0,0,-1)}^{(1)}(\theta_1 \dots \theta_6) - 0.184451 \Psi_{(0,0,1,0,0,-1)}^{(2)}(\theta_1 \dots \theta_6) + 0.05034 \Psi_{(0,0,1,0,0,-1)}^{(2)}(\theta_1 \dots \theta_6) \right).
\end{aligned} \tag{21}$$

The coefficients of each element of the set $\{\theta_1^{a_1} \theta_2^{a_2} \dots \theta_6^{a_6} : a_i \in \mathcal{I}^+, a_1 + \dots + a_6 \leq 3\}$ on the left and right hand side of this expression are equated to form a set of 83 ordinary differential equations. Converting the joint moments to cumulants will close this set of equations, and the numerical solution of such will yield approximations to the elements of the set $\{k_{a_1, \dots, a_6}(t) : a_i \in \mathcal{I}^+, \sum_{i=1}^6 a_i \leq 3\}$. In order to obtain the transient queueing performance measures, we note that

$$E[X_i(t)] = k_{e_i}(t), \quad 1 \leq i \leq 6 \tag{22}$$

where e_i denotes a row vector whose i^{th} element is unity and all other elements are zero. The sortie generation rate corresponds directly to the throughput of node 2 of Figure 2. Therefore, by applying Little's Law at this node, the expected number of sorties generated up to time t , denoted by $E[\Lambda(t)]$, is given by

$$E[\Lambda(t)] := \int_0^t \mu_2 k_{e_2}(t) dt. \tag{23}$$

5 Numerical Example

In this section, we demonstrate the implementation of the procedure described in section 4. In particular, we set up and numerically solve the set of ordinary differential equations given by Eqns. (20) and (21) for a closed queueing network containing ten aircraft (i.e., $N = 10$). As previously noted, the extension of this model to larger values of N will not increase the number of differential equations in this set. To further describe our example problem, we refer to the node indices of Figure 2. We assume that the probability of a pre-sortie ground abort is $p_{14} = 0.05$, and we separately evaluate the model under the probabilities $p_{24} = 0.20, 0.35$ of a post-sortie malfunction. We assume that all aircraft are initially grounded and waiting for taxi at node 1; hence, $k_{e_1}(0) = 10$. All other cumulants are set to zero at time $t = 0$. All numerical results in this section were obtained using the *Mathematica*® computing environment.

For demonstrative purposes, we studied the expected workload and throughput of the network over the transient period which is defined to be the time interval $[0, 40]$. The expected workload at each node corresponds directly to the first order cumulant of $\mathbf{X}(t)$, and the expected throughput, i.e. expected number of sorties flown by time t , may be calculated directly by using Eq. (23). Based on previous empirical testing in Matis [8], first order cumulant approximations under $m = 3$ for high traffic networks of this general topology are relatively tight, i.e. 5%.

The output of our numerical example for the stochastic routing probabilities $p_{14} = 0.05$, $p_{12} = 0.95$, $p_{24} = 0.20$, and $p_{23} = 0.80$ is displayed through Figures (3)-(9). In particular, we have plotted the expected workload and number of sorties flown as a function of time. It is noted that each of these measures approaches a steady-state condition rapidly using the particular parameter values.

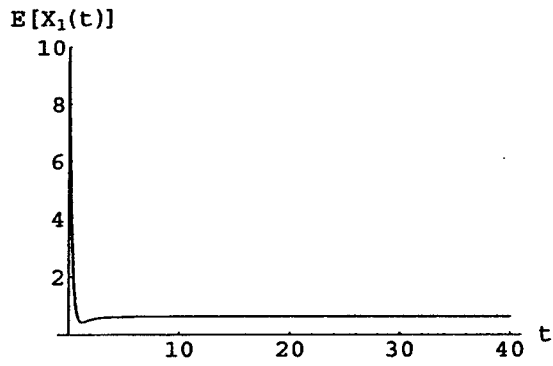


Figure 3: Expected workload at node 1.

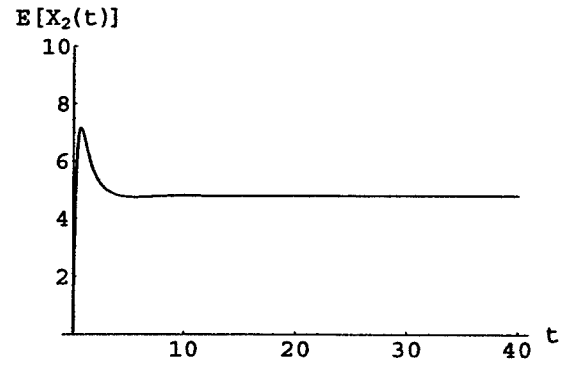


Figure 4: Expected workload at node 2.

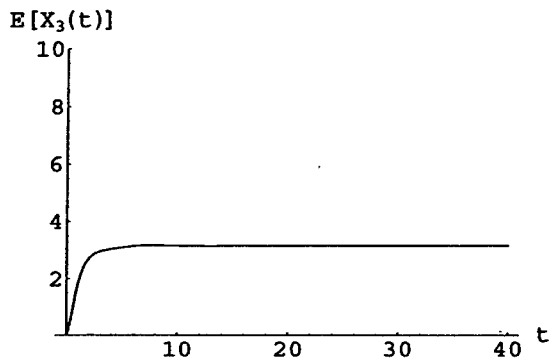


Figure 5: Expected workload at node 3.

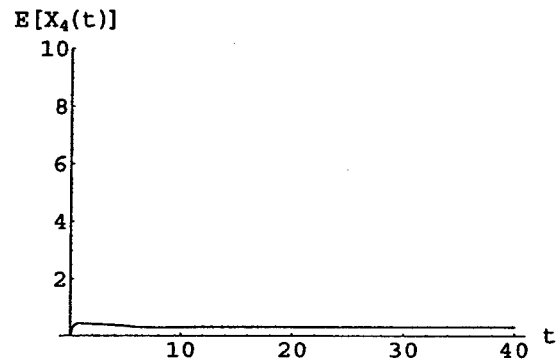


Figure 6: Expected workload at node 4.

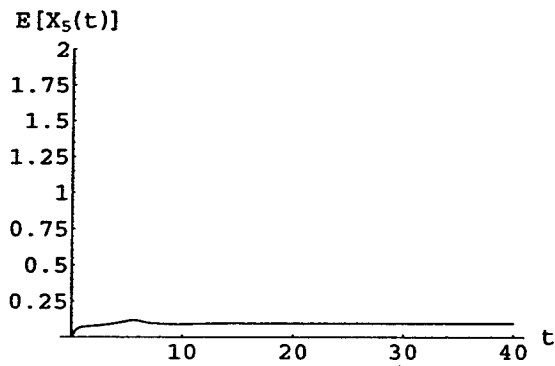


Figure 7: Expected workload at node 5.

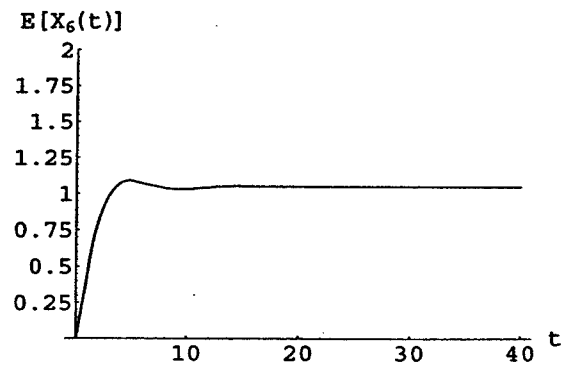


Figure 8: Expected workload at node 6.

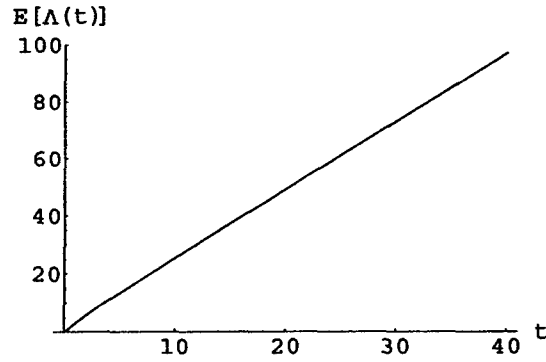


Figure 9: Expected number of sorties by t .

The output of our numerical example for the stochastic routing probabilities $p_{14} = 0.05$, $p_{12} = 0.95$, $p_{24} = 0.35$, and $p_{23} = 0.65$ is displayed through Figures (10)-(17). It is interesting to note the dampened oscillatory patterns of the measures $E[X_i(t)]$ for $i = 5, 6$ corresponding to Figures (14) and (15) respectively. The emergence of this pattern as the probability of a post-sortie malfunction increases is likely due to the network being closed with a limited number of aircraft, the large differences in the parameters $\nu_i(n)$ with n as listed in Table 3, and the truncation of cumulants at $m = 3$. The overall expected holding time of the aircraft $E[X_1(t) + X_2(t)] = E[X_1(t)] + E[X_2(t)]$ of Figure (16) does not oscillate greatly as do the individual nodes, which is typically the measure of practical interest.

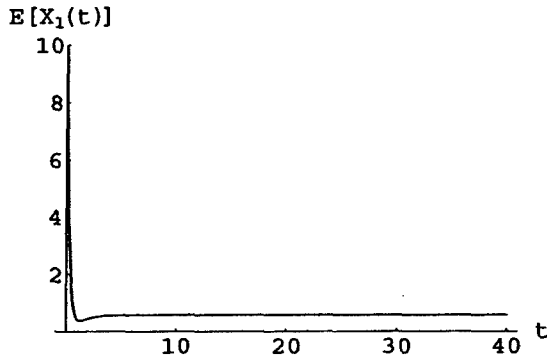


Figure 10: Expected workload at node 1.

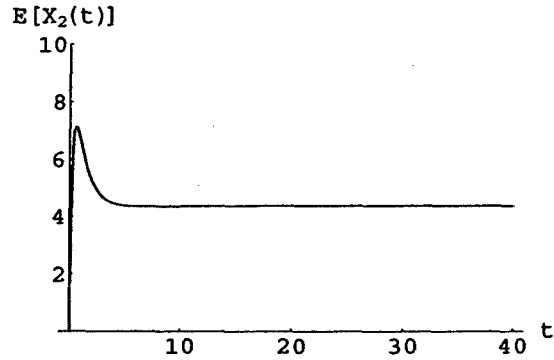


Figure 11: Expected workload at node 2.

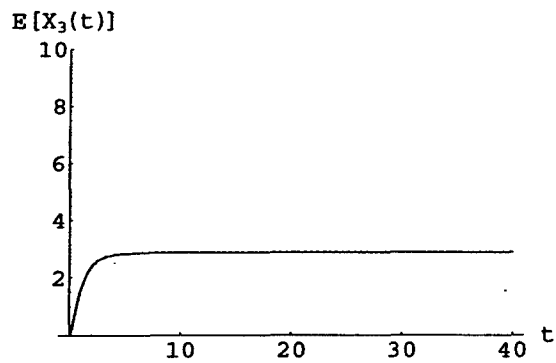


Figure 12: Expected workload at node 3.

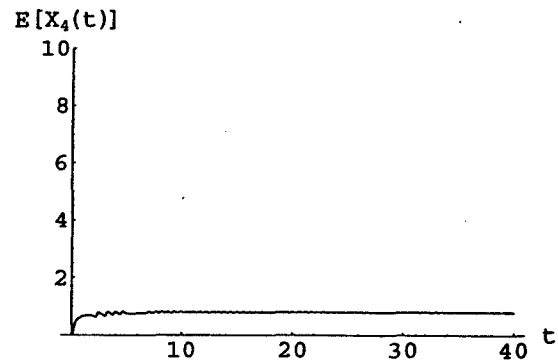


Figure 13: Expected workload at node 4.

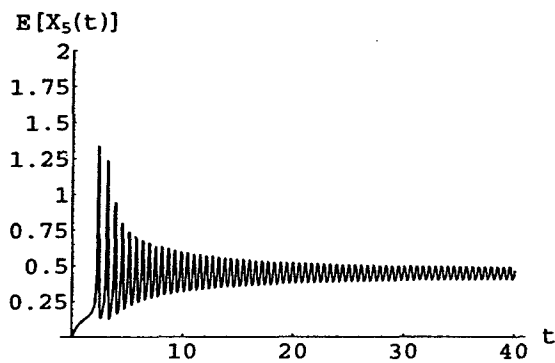


Figure 14: Expected workload at node 5.

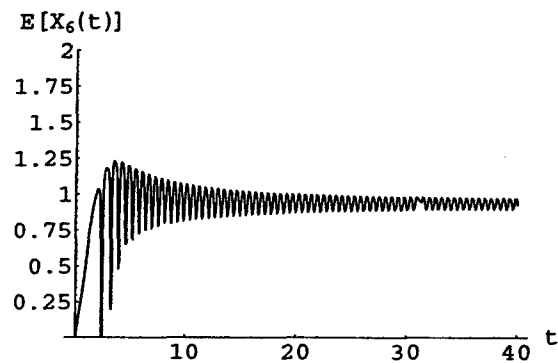


Figure 15: Expected workload at node 6.

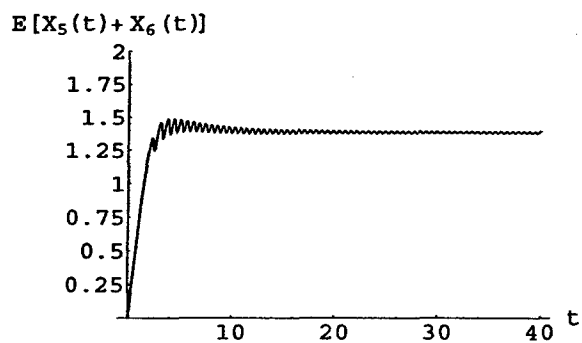


Figure 16: Expected workload (nodes 5 and 6).

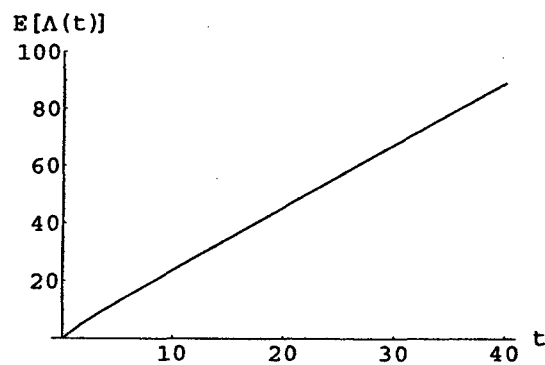


Figure 17: Expected number of sorties by t .

6 Conclusions

This work has considered the important concept of operational readiness for an individual air base, particularly when the measures of operational readiness depend explicitly on time due to theater-level dynamics. This paper has extended a previous queueing network model for the aircraft sortie generation process by solving for vital, time-variant performance measures including the workload in the system as well as the expected number of sorties flown over a transient time period. Moreover, we generalized the maintenance service time distribution by considering a phase-type (PH) representation that accommodates a transient analysis via the method of cumulant functions and allows for inclusion of the likely phenomenon of blocking at the repair hangar. In particular, we assumed that a single repair hangar accommodates at most two aircraft. By adapting and employing the cumulant function method, we obtained a computationally tractable set of ordinary differential equations that are independent of the number of aircraft in the system. Our approach to the problem allows for the computation of mean performance measures as an explicit function of time. Though the cumulant-based procedure for transient analysis was tailored for this queueing network model of the aircraft sortie generation process, it is well suited for other applications in manufacturing, transportation, distribution networks.

References

- [1] Abell, J.B. (1981), *The Sortie Generation Model System*, Logistics Management Institute, Washington, D.C., Sept. 1981.
- [2] Dietz, D.C. and R. Jenkins (1997), Analysis of aircraft sortie generation with the use of a fork-join queueing network model, *Naval Research Logistics* 44, 153-164.
- [3] Fisher, R.R. *et al.* (1968), The Logistics Composite Model: An Overall View, Technical Report No. RM-5544-PR, The Rand Corporation, Santa Monica, CA.
- [4] Kao, E. (1997), *An Introduction to Stochastic Processes*, Duxbury, New York.
- [5] Kendall, M. (1994) *Advanced Theory of Statistics*, Halsted Press, New York.
- [6] Hackman, D.V. and D.C. Dietz (1997) Analytical modeling of aircraft sortie generation with concurrent maintenance and general service times, *Military Operations Research* 3, 61-74.
- [7] Jenkins, R. (1994) *A Mean Value Analysis Heuristic for Analysis of Aircraft Sortie Generation*. M.S. Thesis, Air Force Institute of Technology, Wright Patterson AFB, OH.
- [8] Matis, T. (2001) *Using Cumulant Functions in Queueing Theory*, Ph.D. Dissertation, Texas A&M University, College Station, Texas.
- [9] Matis, T. and R. Feldman (2001), Transient analysis of state-dependent queueing networks via cumulant functions, *Journal of Applied Probability* 38, 841-859.
- [10] Neuts, M. (1981), *Matrix-Geometric Solutions in Stochastic Models: An Algorithmic Approach*, Johns Hopkins University Press, Baltimore.
- [11] Rao, P.C., and R. Suri (1994) Approximate queueing network models for closed fabrication/assembly systems. Part I: Single-level systems, *Production and Operations Management*, 4, 244-275.